Coded OFDM-IM With Transmit Diversity

Jinho Choi

***Abstract*— In this paper, we propose a simple transmit diversity scheme for orthogonal frequency division multiplexing (OFDM) with index modulation (IM) in order to achieve a diversity gain for index detection, which can significantly improve the performance of OFDM-IM at the cost of the spectral efficiency. An optimal approach for active index detection is derived, which has a complexity, growing linearly with the size of OFDM symbol. A salient feature of the proposed transmit diversity scheme is that it can be easily employed in conjunction with a conventional coding scheme for data symbols. Consequently, we can implement coded OFDM-IM together with the proposed transmit diversity scheme in a straightforward manner, which can provide a good performance under a frequency-fading environment.**

***Index Terms*— Index modulation, orthogonal frequency division multiplexing, diversity, performance analysis.**

I. Introduction

THE NOTION of index modulation (IM) has been introduced for multiple-input multiple-output (MIMO) systems in [1] (see also [2], [3] for a comprehensive overview) to convey information bits by the indices of active transmit antennas. The resulting modulation technique is called spatial modulation (SM), which is shown to be energy efficient and has a low implementation cost. In [4], an optimal detection for SM is studied with its performance analysis. SM has been extended with channel coding [5], [6] and some modifications [7], [8].

The notion of IM is also adopted in orthogonal frequency division multiplexing (OFDM) in [9] and [10], where a subset of subcarriers are active and the indices of them are used to convey additional information bits. The resulting modulation scheme is called OFDM-IM. An overview of various IM techniques is presented in [11]. In [12], a performance analysis is carried out when a maximum likelihood (ML) detector is employed. There are various generalizations of OFDM-IM. For example, in [13], the number of active subcarriers is not fixed to increase the spectral efficiency; in [14], OFDM-IM is applied to MIMO systems. In [15], the optimal number of active subcarriers is studied to improve the spectral efficiency as well as energy efficiency.

Provided that there are a few active transmit antennas in SM or subcarriers in OFDM-IM, the notion of compressive sensing (CS) [16], [17] can be adopted to design low-complexity detectors. For example, CS based detectors are studied for SM in [18] and [19] and for OFDM-IM in [20].

Manuscript received October 8, 2016; revised January 17, 2017, March 6, 2017, and April 20, 2017; accepted April 23, 2017. Date of publication April 27, 2017; date of current version July 13, 2017. This work was supported by the GIST Research Institute (GRI) in 2017. The associate editor coordinating the review of this paper and approving it for publication was C.-X. Wang.

The author is with School of Electrical Engineering and Computer Science, Gwangju Institute of Science and Technology, Gwangju 61005, South Korea (e-mail: jchoi0114@gist.ac.kr).

Digital Object Identifier 10.1109/TCOMM.2017.2699182

Unlike SM, OFDM-IM has a poor performance under fading. This is a weakness of OFDM-IM inherited from OFDM, which cannot exploit any diversity gain under a frequency-selective fading channel environment [21], [22]. In order to improve the performance of OFDM-IM, MIMO can be considered for OFDM-IM as in [14]. It is also possible to consider a transmit diversity scheme without using multiple antennas as in [23].

It is noteworthy that channel coding plays a crucial role in improving the performance of OFDM systems under a frequency-selective fading channel environment [24]. Together with interleaving, the path diversity gain can be exploited by channel coding in coded OFDM and a good performance can be achieved without losing the main advantages of OFDM (e.g., low-complexity one-tap equalization). However, unlike coded OFDM, it is clearly shown in [23] that the direct application of channel coding to OFDM-IM cannot result in a good performance unless a transmit diversity scheme is used.

The transmit diversity scheme in [23] is based on the signal-space diversity scheme studied in [25] for MIMO systems. Although it might be possible to employ any signal-space diversity schemes for OFDM-IM, an orthogonal design is desirable to keep the complexity of detector low. From this point of view, in [23], only one orthogonal design that can provide a diversity gain of 2 is considered.

In this paper, we propose a simple but effective transmit diversity scheme for OFDM-IM. The main features of the proposed transmit diversity scheme are as follows: *i*) it can provide any diversity order; *ii*) the complexity of an optimal approach for active index detection is linear in the size of signal block (or OFDM symbol); *iii*) it can be easily used in conjunction with a conventional coding scheme for data symbols. Due to the above features, the proposed transmit diversity scheme becomes attractive to improve the performance of OFDM-IM without any significant computational complexity increase at the transmitter and receiver.

The rest of the paper is organized as follows. In Section II, a system model is presented for OFDM-IM. The transmit diversity scheme proposed in [23] is discussed in Section III. A simple transmit diversity scheme for OFDM-IM is proposed in Section IV, where the ML approach for active index detection is also derived. In Section V, simulation results are presented. The paper is finally concluded in Section VI with some remarks.

A. Notation

Matrices and vectors are denoted by upper- and lower-case boldface letters, respectively. The superscripts T and H denote the transpose and complex conjugate, respectively. The p-norm of a vector $\mathbf{a}$ is denoted by $\|\mathbf{a}\|_p$ (If $p = 2$, the norm is

denoted by $||\mathbf{a}||$ without the subscript). For a vector $\mathbf{a}$, diag($\mathbf{a}$) is the diagonal matrix with the diagonal elements from $\mathbf{a}$. For a matrix $\mathbf{X}$ (a vector $\mathbf{a}$), $[\mathbf{X}]_n$ ($[\mathbf{a}]_n$) represents the nth column (element, resp.). If n is a set of indices, $[\mathbf{X}]_n$ is a submatrix of $\mathbf{X}$ obtained by taking the corresponding columns. $\mathbb{E}[\cdot]$ and $\mathrm{Var}(\cdot)$ denote the statistical expectation and variance, respectively. $\mathcal{CN}(\mathbf{a}, \mathbf{R})$ ($\mathcal{N}(\mathbf{a}, \mathbf{R})$) represents the distribution of circularly symmetric complex Gaussian (CSCG) (resp., real-valued Gaussian) random vectors with mean vector $\mathbf{a}$ and covariance matrix $\mathbf{R}$.

II. System Model

Suppose that a block of B subcarriers is divided into K subblock of L subcarriers, i.e., $B = KL$, in an OFDM system. For each subblock, there are G clusters of N subcarriers (i.e., $L = GN$). Let

$$\mathbf{x}_k = [\mathbf{s}_{k;0}^{\mathrm{T}} \ \cdots \ \mathbf{s}_{k;G-1}^{\mathrm{T}}]^{\mathrm{T}}$$

denote the kth subblock of data symbols to be transmitted, where $\mathbf{s}_{k;g}$ denotes the signal vector of size $N \times 1$ transmitted through the gth cluster within the kth subblock. We assume that there are Q active subcarriers per cluster for IM, where an active subcarrier means a subcarrier that transmits a data symbol with non-zero transmission power. That is,

$$||\mathbf{s}_{k;g}||_0 = Q,$$

as the transmission power of inactive subcarriers is zero. For convenience, denote by $I_{k;g}$ the index set of the active subcarriers or the support[1] of $\mathbf{s}_{k;g}$. A non-zero element of $\mathbf{s}_{k;g}$ (or an element corresponding to an active subcarrier) is an element of the signal constellation, denoted by $\mathcal{S}$. We assume that $|\mathcal{S}| = M$ for M-ary modulation and $\mathcal{S}$ does not include zero, i.e., $0 \notin \mathcal{S}$.

For the transmission of each block, a cyclic prefix (CP) is appended to the OFDM symbol,

$$\mathbf{x} = [\mathbf{x}_0^{\mathrm{T}} \ \cdots \ \mathbf{x}_{K-1}^{\mathrm{T}}]^{\mathrm{T}}.$$

At the receiver after removing the signal part corresponding to CP, we have the following received signal vector of size $B \times 1$:

$$\mathbf{y} = \mathcal{H}\mathbf{x} + \mathbf{n}, \tag{1}$$

where $\mathbf{n} \sim \mathcal{CN}(\mathbf{0}, N_0\mathbf{I})$ is the background noise vector and $\mathcal{H}$ is the frequency-domain channel matrix that is given by

$$\mathcal{H} = \mathrm{diag}(H_0 \ \cdots \ H_{B-1}).$$

Here, H_i represents the (frequency-domain) channel coefficient of the ith subcarrier. Then, the number of information bits per subblock becomes

$$N_{\mathrm{b}} = G\left(\lfloor \log_2 \binom{N}{Q} \rfloor + Q \log_2 M\right). \tag{2}$$

The resulting system is called OFDM-IM for $G = 1$ [10]. For convenience, the information bits transmitted by IM are referred to as index-modulated or IM bits. Note that the structure of OFDM symbol in this section has been modified from that[2] in [10] in order to accommodate a transmit diversity scheme that will be explained in Section IV.

[1]The support of a vector is the index set of non-zero elements.

[2]In [10], $G = 1$, i.e., cluster is equivalent to subblock.

III. An Existing Diversity Scheme for OFDM-IM

In [12], the performance of OFDM-IM is analyzed when $Q = 1$. It is clearly shown that the diversity order of OFDM-IM is 1. Thus, the performance cannot be significantly improved by increasing the signal-to-noise ratio (SNR). To exploit the diversity gain for better performance, in [23], interleaving within a cluster, which is called coordinated interleaving (CI), is employed so that a data symbol can be transmitted through multiple subcarriers. In this section, we present this transmit diversity scheme.

To discuss the transmit diversity scheme in [23], we consider a particular example. Let $N = 4$ and $Q = 2$. In addition, we assume that $K = 1$ (i.e., the number of subblocks is 1) and omit the subblock index k for convenience. In this case, the number of IM bits per cluster is $\lfloor \log_2 \binom{4}{2} \rfloor = 2$. Thus, there are four possible combinations for IM per cluster. Denote by $\mathbf{a}_g$ the IM bits for cluster g. Then, we can consider the following combinations of active subcarriers within a cluster:

$$\begin{aligned}
\mathbf{a}_g &= [0\ 0]^{\mathrm{T}} \Rightarrow I_g = \mathrm{supp}(\mathbf{s}_g) = \{0, 2\} \\
\mathbf{a}_g &= [0\ 1]^{\mathrm{T}} \Rightarrow I_g = \mathrm{supp}(\mathbf{s}_g) = \{1, 3\} \\
\mathbf{a}_g &= [1\ 0]^{\mathrm{T}} \Rightarrow I_g = \mathrm{supp}(\mathbf{s}_g) = \{0, 3\} \\
\mathbf{a}_g &= [1\ 1]^{\mathrm{T}} \Rightarrow I_g = \mathrm{supp}(\mathbf{s}_g) = \{1, 2\}.
\end{aligned}$$

Let s_1 and s_2 be the data symbols in a rotated signal constellation, denoted by $\mathcal{S}_\theta$, where θ represents the angle of rotation, to be transmitted within a cluster. Then, for CI, according to [23], we have the following mapping:

$$\begin{aligned}
\mathbf{s}_g &= \mathcal{M}(s_1, s_2; \mathbf{a}_g) \\
&\in \left\{ \begin{array}{l}
[\Re(s_1) + j\Im(s_2)\ 0\ \Re(s_1) + j\Im(s_2)\ 0]^{\mathrm{T}}, \\
[0\ \Re(s_1) + j\Im(s_2)\ 0\ \Re(s_1) + j\Im(s_2)]^{\mathrm{T}}, \\
[\Re(s_1) + j\Im(s_2)\ 0\ 0\ \Re(s_1) + j\Im(s_2)]^{\mathrm{T}}, \\
[0\ \Re(s_1) + j\Im(s_2)\ \Re(s_1) + j\Im(s_2)\ 0]^{\mathrm{T}}
\end{array} \right\},
\end{aligned}$$

where $\Re(x)$ and $\Im(x)$ represent the real and imaginary parts of x, respectively, and $j = \sqrt{-1}$. A single data symbol, say s_1, can be transmitted through two different subcarriers (e.g., the 0th and 1st subcarriers within a cluster). Thus, the diversity gain can be 2. This example is based on an orthogonal design in [25] and allows a detection complexity that grows linearly with Q.

If we assume $G = 1$ for the sake of simplicity, the following joint detection can be considered [23]:

$$\min_{s_1, s_2 \in \mathcal{S}_\theta, I} ||[\mathbf{y}]_I - [\mathcal{H}]_I \mathcal{M}(s_1, s_2; \mathbf{a})||^2, \tag{3}$$

where I is the index set of active subcarriers and $[\mathbf{y}]_I$ and $[\mathcal{H}]_I$ represent the subvector of $\mathbf{y}$ and the submatrix of $\mathcal{H}$ corresponding to the elements and columns in I, respectively. With $N = 4$ and $Q = 2$, we have

$$I \in \{\{0, 2\}, \{1, 3\}, \{0, 3\}, \{1, 2\}\}$$

as mentioned earlier, and $[\mathbf{y}]_{I=\{0,2\}} = [y_0\ y_2]^{\mathrm{T}}$. It can be shown that

$$[\bar{\mathbf{y}}]_I = \begin{bmatrix} \Re([\mathbf{y}]_I) \\ \Im([\mathbf{y}]_I) \end{bmatrix} = [\bar{\mathcal{H}}]_I \begin{bmatrix} \Re(s_1) \\ \Im(s_1) \\ \Re(s_2) \\ \Im(s_2) \end{bmatrix} + \begin{bmatrix} \Re([\mathbf{n}]_I) \\ \Im([\mathbf{n}]_I) \end{bmatrix}.$$

Due to the orthogonal design, we can have $[\bar{\mathcal{H}}]_I = [[\bar{\mathcal{H}}_{(1)}]_I\ [\bar{\mathcal{H}}_{(2)}]_I]$, where $[\bar{\mathcal{H}}_{(1)}]_I$ and $[\bar{\mathcal{H}}_{(2)}]_I$ are orthogonal for each I. From this, the joint detection problem in (3) can be reduced to

$$\min_{I}\left\{\min_{s_1\in\mathcal{S}_\theta}||[\bar{\mathbf{y}}]_I-[\bar{\mathcal{H}}_{(1)}]_I\begin{bmatrix}\Re(s_1)\\ \Im(s_1)\end{bmatrix}||^2 + \min_{s_2\in\mathcal{S}_\theta}||[\bar{\mathbf{y}}]_I-[\bar{\mathcal{H}}_{(2)}]_I\begin{bmatrix}\Re(s_2)\\ \Im(s_2)\end{bmatrix}||^2\right\}, \tag{4}$$

which has a complexity proportional to $2M$, not M^2, as explained in [23].

We have few remarks as follows.

- The above approach with $Q = 2$ can achieve a diversity order of 2 for the data symbol detection. For convenience, this approach is considered for the performance comparison in this paper and referred to as CI-OFDM-IM.
- In addition to CI, if data symbols are coded symbols, a better performance can be achieved with a higher diversity gain as demonstrated in [23].

IV. A Transmit Diversity Scheme for IM and Active Index Detection

In this section, we propose a simple transmit diversity scheme for OFDM-IM and derive the ML approach for active index detection. In addition, we obtain soft decisions for the coded bits that are transmitted through active subcarriers.

A. OFDM-IM With Transmit Diversity

In general, if the support of $\mathbf{s}_{k;g}$ is erroneously detected, the data symbols of active subcarriers cannot be correctly decided. Thus, the performance of OFDM-IM is mainly decided by the detection performance of active subcarriers. For a better performance of active index (or IM bits) detection, we may need to use a transmit diversity scheme for OFDM-IM. In Fig. 1, an illustration of the transmitter structure for OFDM-IM is shown with the proposed transmit diversity scheme, which will be explained in detail in Subsection IV-B. In this transmit diversity scheme, the same set of active subcarriers is used for all clusters within a subblock. Note that throughout the paper, we assume that the non-zero data symbols in $\mathbf{s}_{k;g}$ transmitted through active subcarriers are coded as shown in Fig. 1.

It is noteworthy that the resulting system is relatively simple as channel coding can be independently applied to the data symbols that are to be transmitted through active subcarriers, while the IM bits are uncoded. However, although no channel coding is used for IM bits, we can show that the detection performance of IM bits or active subcarriers can be significantly improved by the proposed simple transmit diversity scheme.

B. The Proposed Transmit Diversity Scheme

Without loss of generality, we focus on the received signal subvector corresponding to a subblock. From (1), let

$$\mathbf{y}_k = \mathcal{H}_k\mathbf{x}_k + \mathbf{n}_k, \tag{5}$$

where $\mathbf{y}_k$ is the kth subvector of $\mathbf{y}$, $\mathcal{H}_k$ is the kth submatrix of $\mathcal{H}$, and $\mathbf{n}_k$ is the kth subvector of $\mathbf{n}$. For convenience, we

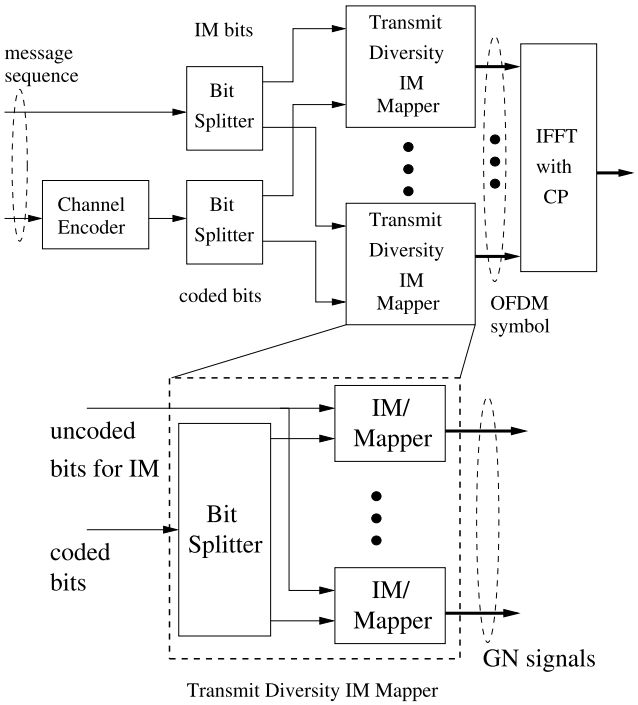

Fig. 1. An illustration of the transmitter for coded OFDM-IM with a transmit diversity scheme.

omit the subblock index k in this section. As illustrated in Fig. 1, in order to obtain a transmit diversity gain, we consider the same support for all the $\mathbf{s}_g$'s within a subblock, i.e.,

$$I_g = I, \quad g = 0, \ldots, G-1,$$

while the data symbols of active subcarriers in each $\mathbf{s}_g$ are still independent. In this case, the number of bits per subblock becomes

$$\bar{N}_{\mathrm{b}} = \lfloor \log_2 \binom{N}{Q} \rfloor + GQ\log_2 M, \tag{6}$$

which is smaller than that of conventional OFDM-IM in (2) as the number of IM bits is reduced from $G\lfloor \log_2 \binom{N}{Q} \rfloor$ to $\lfloor \log_2 \binom{N}{Q} \rfloor$. The resulting system with the above transmit diversity scheme is referred to as OFDM-IM with transmit diversity (OFDM-IM-TD) in this paper.

In Fig. 2, we show the number of bits per subblock for various values of G when $L = 128$ and $M = 4$. Clearly, the number of bits per subblock of OFDM-IM-TD is smaller than that of OFDM-IM. It is interesting to note that the number of bits per subblock increases with G when Q is fixed. Although OFDM-IM-TD has a smaller number of bits per subblock than OFDM-IM, we will show that its performance is much better than that of OFDM-IM (and CI-OFDM-IM) over fading channels as the performance of active index detection can be significantly improved for a large G.

Note that in OFDM-IM-TD, the number of bits per block is given by

$$K\bar{N}_{\mathrm{b}} = K\left(\lfloor \log_2 \binom{\frac{B}{KG}}{Q} \rfloor + GQ\log_2 M\right). \tag{7}$$

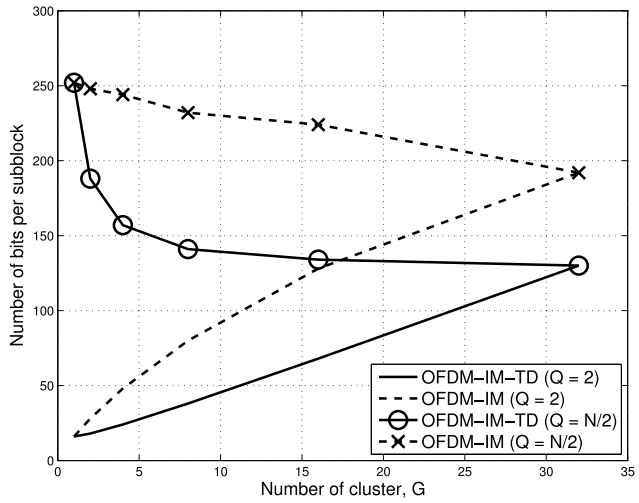

Fig. 2. The number of bits per subblock for different values of G when $L = 128$ and $M = 4$.

This shows that when B, G, Q, and M are fixed, the number of bits per block increases with K. That is, it is desirable to have a larger K to transmit more bits per block or increase the spectral efficiency.

C. ML Approach for Active Index Detection

At the receiver in OFDM-IM-TD, the estimation of I is to be carried out in the first step. Once I is estimated, the data symbols corresponding to I in each cluster are to be detected in the second step. In this subsection, we focus on the first step for active index detection or the estimation of I.

Let $\mathbf{r}_{k;g}$, $\mathbf{n}_{k;g}$, and $\mathbf{H}_{k;g}$ denote the gth subvectors of $\mathbf{y}_k$ and $\mathbf{n}_k$, and the submatrix of $\mathcal{H}_k$ in (5) corresponding to $\mathbf{s}_{k;g}$, respectively. Here, for convenience, we also omit the subblock index k. In OFDM-IM-TD, since $I_g = I$ for all g, I has to be detected from all $\mathbf{r}_g$'s. Thus, the ML detection for I can be formulated as

$$\max_{I,[\mathbf{s}_g]_I \in \mathcal{S}^Q} \prod_{g=0}^{G-1} f(\mathbf{r}_g | I, \mathbf{s}_g) = \min_{I} \sum_{g=0}^{G-1} \left(\min_{[\mathbf{s}_g]_I \in \mathcal{S}^Q} ||[\mathbf{r}_g - \mathbf{H}_g \mathbf{s}_g]_I||^2 + ||[\mathbf{r}_g]_{I^c}||^2 \right), \tag{8}$$

where

$$f(\mathbf{r}_g \mid I, \mathbf{s}_g) = \frac{1}{(\pi N_0)^L} e^{-\frac{1}{N_0}\left(||[\mathbf{r}_g - \mathbf{H}_g \mathbf{s}_g]_I||^2 + ||[\mathbf{r}_g]_{I^c}||^2\right)}.$$

A low-complexity implementation for the ML detection can be obtained by the following approach.

For each subcarrier within a cluster, consider the following two hypotheses:

$$\begin{aligned} &\mathsf{H}_0 : \ r_{g,m} = n_{g,m}, \quad \forall g; \\ &\mathsf{H}_1 : \ r_{g,m} = H_{g,m} s_{g,m} + n_{g,m}, \quad s_{g,m} \in \mathcal{S}, \ \forall g, \end{aligned} \tag{9}$$

where $r_{g,m}$, $H_{g,m}$, and $n_{g,m}$ are the gth elements of $\mathbf{r}_g$, $\mathbf{H}_g$, and $\mathbf{n}_g$, respectively. Clearly, H_0 and H_1 are the hypotheses of the absence and presence of signal for each m, respectively. Let $\mathbf{v}_m = [r_{0,m} \ \ldots \ r_{G-1,m}]^{\mathrm{T}}$. Under H_i, denote by $f_i(\mathbf{v}_m)$ the distribution of $\mathbf{v}_m$. Then, under H_0, we have

$$\begin{aligned} f_0(\mathbf{v}_m) &= \prod_{g=0}^{G-1} \frac{1}{\pi N_0} e^{-\frac{|r_{g,m}|^2}{N_0}} \\ &= \frac{1}{(\pi N_0)^G} e^{-\frac{||\mathbf{v}_m||^2}{N_0}}. \end{aligned} \tag{10}$$

Under H_1, if $s_{g,m}$, $g = 0, \ldots, G-1$, is known, we have

$$f_1(\mathbf{v}_m) = \prod_{g=0}^{G-1} \frac{1}{\pi N_0} e^{-\frac{|r_{g,m} - H_{g,m} s_{g,m}|^2}{N_0}}. \tag{11}$$

However, $s_{g,m}$, $g = 0, \ldots, G-1$, is unknown. Thus, the distribution of $\mathbf{v}_m$ under H_1 can be replaced with the following [26]:

$$\begin{aligned} f_1(\mathbf{v}_m) &= \prod_{g=0}^{G-1} \max_{s_{g,m} \in \mathcal{S}} \frac{1}{\pi N_0} e^{-\frac{|r_{g,m} - H_{g,m} s_{g,m}|^2}{N_0}} \\ &= \frac{1}{(\pi N_0)^G} e^{-\sum_{g=0}^{G-1} \frac{\Delta_{g,m}}{N_0}}, \end{aligned} \tag{12}$$

where $\Delta_{g,m} = \min_{s_{g,m} \in \mathcal{S}} |r_{g,m} - H_{g,m} s_{g,m}|^2$. For the generalized likelihood ratio test (GLRT), let the log-likelihood ratio (LLR) of the mth subcarrier in each cluster be

$$\eta_m = \log \frac{f_1(\mathbf{v}_m)}{f_0(\mathbf{v}_m)} = \frac{1}{N_0} \left(||\mathbf{v}_m||^2 - \sum_{g=0}^{G-1} \Delta_{g,m} \right). \tag{13}$$

For each m, we can accept H_0 if $\eta_m < 0$. Otherwise, we accept H_1. This approach has a complexity order proportional to N, while it is not optimal as the constraint of $|I| = Q$ is not imposed. However, we can show that the ML detection of I in (8) can be carried out with η_m as follows.

Theorem 1: The solution to the ML problem in (8) *is given by*

$$\hat{I} = \{m(1), \ldots, m(Q)\}, \tag{14}$$

where $\eta_{m(1)} \geq \ \ldots \ \geq \eta_{m(N)}$. *That is,* $m(q)$ *denotes the* q*th largest LLR.*

Proof: From (8), the ML detection of I is to maximize $\prod_{g=0}^{G-1} \max_{\mathbf{s}_g \in \mathcal{S}^Q} f(\mathbf{r}_g \mid I, \mathbf{s}_g)$. Since $\prod_{g=0}^{G-1} f(\mathbf{r}_g \mid I = \emptyset)$ is constant with respect to I, the ML solution to decide I is to maximize the following ratio:

$$\frac{\prod_{g=0}^{G-1} \max_{\mathbf{s}_g \in \mathcal{S}^Q} f(\mathbf{r}_g \mid I, \mathbf{s}_g)}{\prod_{g=0}^{G-1} f(\mathbf{r}_g \mid I = \emptyset)} = \frac{\prod_{m \in I} f_1(\mathbf{v}_m)}{\prod_{m \in I} f_0(\mathbf{v}_m)}, \tag{15}$$

because

$$\begin{aligned} \prod_{g=0}^{G-1} \max_{\mathbf{s}_g \in \mathcal{S}^Q} f(\mathbf{r}_g \mid I, \mathbf{s}_g) &= \prod_{m \in I} f_1(\mathbf{v}_m) \prod_{m \in I^c} f_0(\mathbf{v}_m) \\ \prod_{g=0}^{G-1} f(\mathbf{r}_g \mid I = \emptyset) &= \prod_{m \in I} f_0(\mathbf{v}_m) \prod_{m \in I^c} f_0(\mathbf{v}_m). \end{aligned}$$

Thus, taking the logarithm, the ML detection can be re-formulated as

$$\hat{I} = \underset{I}{\operatorname{argmax}} \sum_{m \in I} \eta_m. \tag{16}$$

Since $|I| = Q$, the ML solution can be found by the Q largest η_m's as in (14). ■

The complexity to perform the ML approach for active index detection is dependent on that to find η_m in (13). For each m, since the complexity order to decide $\Delta_{g,m}$ is $O(M)$, the complexity order to find η_m is $O(GM)$. Thus, for each subblock, to find all the η_m's, the complexity order becomes $O(NGM) = O(LM)$. This demonstrates that the complexity to perform the ML approach for active index detection is linearly proportional to the number of subcarriers or the size of OFDM symbol.

D. Soft Decision for Data Symbols

The ML detection in (8) can also provide the ML decision of the data symbols of active subcarriers, which are hard decisions. However, it is desirable to have soft decisions such as LLRs of data symbols for the input to a channel decoder. According to the structure of the transmitter in Fig. 1, we can consider soft decisions of data symbols or their bits for given estimated I or detected IM bits. That is, once I is detected, we assume that this provides the correct support of $\mathbf{s}_g$ and find LLR values of the bits of the data symbols of active subcarriers. Let

$$\begin{aligned}\mathbf{u}_g &= [u_{g,0} \ \ldots \ u_{g,Q-1}]^{\mathrm{T}} \\ &= [\mathbf{s}_g]_I \in \mathcal{S}^Q.\end{aligned}$$

Then, each $u_{g,q}$ consists of $\log_2 M$ coded bits. Let $\mathcal{S}_{b,i}$ denote the sub-constellation of $\mathcal{S}$ corresponding to bit b among $\log_2 M$ bits when bit b is $i \in \{0, 1\}$. Clearly, we have $\cup_b(\mathcal{S}_{b,0} \cup \mathcal{S}_{b,1}) = \mathcal{S}$.

Let $r_{g,(q)}$ and $H_{g,(q)}$ denote the received signal among the elements of $\mathbf{r}_g$ and the diagonal elements of $\mathbf{H}_g$ corresponding to the qth active subcarrier, respectively. Then, for given $u_{g,q}$, since

$$r_{g,(q)} \sim \mathcal{CN}(H_{g,(q)}u_{g,q}, N_0), \tag{17}$$

the LLR of bit b of $u_{g,q}$ is given by

$$\begin{aligned}\mathrm{LLR}_{g,q,b} &= \log \frac{f(r_{g,(q)}|\langle u_{g,q}\rangle_b = 0)}{f(r_{g,(q)}|\langle u_{g,q}\rangle_b = 1)} \\ &= \frac{\sum_{s\in\mathcal{S}_{b,0}} \exp\left(-\frac{|r_{g,(q)}-H_{g,(q)}s|^2}{N_0}\right)}{\sum_{s\in\mathcal{S}_{b,1}} \exp\left(-\frac{|r_{g,(q)}-H_{g,(q)}s|^2}{N_0}\right)},\end{aligned} \tag{18}$$

where $\langle u\rangle_b$ denotes the bth bit of data symbol u. The LLR values become the input to a channel decoder. As in [22] and [24], the diversity gain depends on the channel code and is usually proportional to the minimum distance of the channel code.

As mentioned earlier, the resulting receiver has two steps. In the first step, the detection of I is carried out. Once I is estimated, the LLR values of coded bits are obtained for decoding.

Without channel coding, although a low IER can be achieved by the proposed transmit diversity scheme in OFDM-IM, the overall performance can be poor as data symbols can experience independent fading. Thus, to obtain the diversity gain for data symbols, $[\mathbf{s}_g]_I$, as mentioned earlier, we consider coded OFDM-IM in this paper as illustrated in Fig. 1. In particular, we consider bit-interleaved coded modulation (BICM) [27], where the soft decision using the LLR in (18) becomes the input to a channel decoder. Note that in this case, in Fig. 1, we need to include the bit interleaver after the channel encoder.

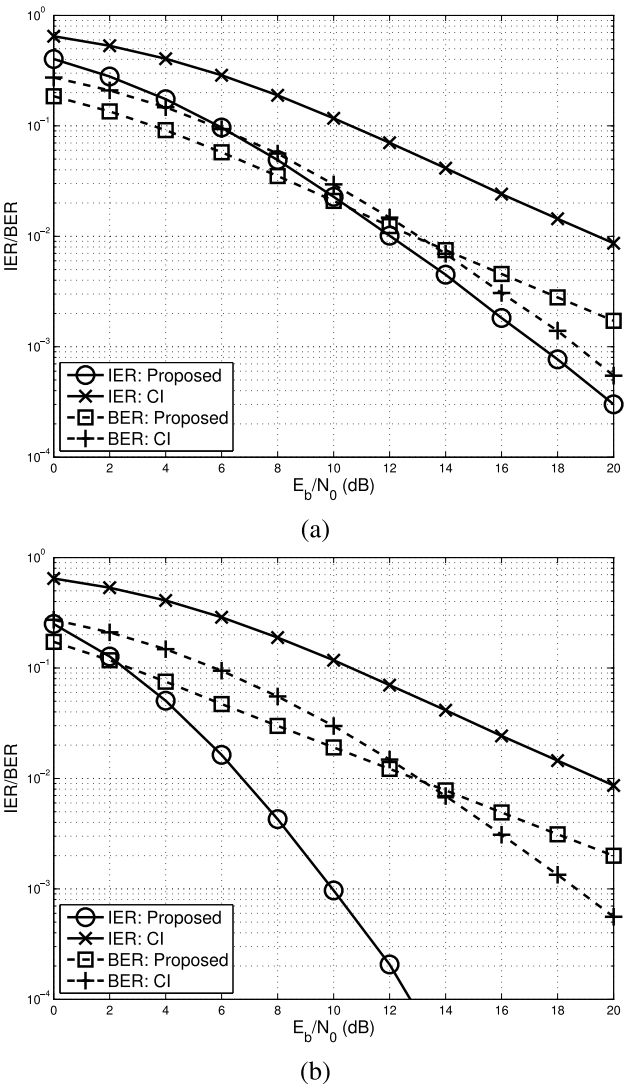

Fig. 3. IER and BER in terms of $\frac{E_b}{N_0}$ when $N = 4$, $Q = 2$, and $M = 4$: (a) $G = 1$; (b) $G = 2$.

V. Simulation Results

In this section, for simulations, we assume 4-quadrature amplitude modulation (QAM) or quadrature phase-shift keying (QPSK) with Gray mapping. Thus, we have $M = 4$ in all simulation results. For a fair comparison, we will consider the same $\frac{E_b}{N_0}$, where E_b denotes the (uncoded) bit energy, for CI-OFDM-IM [23] and OFDM-IM-TD. In particular, E_b is given by

$$E_b = \frac{QE_s}{\text{Number of bits per subblock}},$$

where E_s is the symbol energy, which is given by

$$E_s = \mathbb{E}[|s|^2] = \frac{1}{M}\sum_{s\in\mathcal{S}} |s|^2.$$

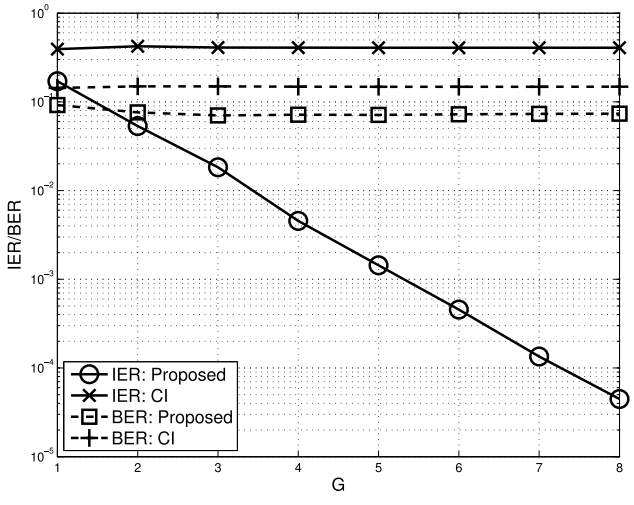

Fig. 4. IER and BER in terms of G when $N = 4$, $\frac{E_b}{N_0} = 4$ dB, $Q = 2$, and $M = 4$.

To generate the channel coefficients, we assume that the $H_{g,m}$'s are independent and

$$H_{g,m} \sim \mathcal{CN}(0, \sigma_H^2),$$

where $\sigma_H^2 = 1$ for normalization. This assumption is also considered in [10], [12], [13], and [23].

A. Performance Comparisons With CI-OFDM-IM

In this subsection, we present simulation results of CI-OFDM-IM and the proposed scheme, i.e., OFDM-IM-TD, to compare their performances in terms of IER for index detection and bit error rate (BER) for data symbol detection.

Fig. 3 shows the IER (of index bits) and BER (of data symbols) of CI-OFDM-IM (in the legend, it is represented by "CI") and the proposed scheme (i.e., OFDM-IM-TD) for various values of SNR, $\frac{E_b}{N_0}$, when the number of subcarriers per cluster, N, is 4, the number of active subcarriers per cluster, Q, is 2, and the size of signal constellation, M, is 4. Note that the BER results in this subsection are based on the conditional BER[3] provided that the active indices are correctly detected). For CI-OFDM-IM, the rotation angle is set to 15°. With $(N, Q) = (4, 2)$, the numbers of bits per subblock of OFDM-IM-TD and CI-OFDM-IM are $2(1+2G)$ and $6G$, respectively. Thus, when $G = 1$, the spectral efficiency of OFDM-IM-TD is the same as that of CI-OFDM-IM. The simulation results with $G = 1$ are shown in Fig. 3 (a). We can see that OFDM-IM-TD performs better than CI-OFDM-IM in terms of IER, while CI-OFDM-IM has a lower BER than OFDM-IM-TD at a high SNR due to a higher diversity gain. It is interesting to observe that the diversity gain of OFDM-IM-TD for index detection seems higher than $G = 1$.

In Fig. 3 (b), the simulation results with $G = 2$ are presented with $N = 4$, $Q = 2$, and $M = 4$ to show the IER and BER of OFDM-IM-TD. From the IER curve, we can confirm that a large diversity gain for index detection is achieved, which leads to a better IER performance than that of of CI-OFDM-IM. In particular, OFDM-IM-TD can have more than 8 dB gain in terms of $\frac{E_b}{N_0}$ at an IER of 10^{-1} (and about 13 dB gain at an IER of 10^{-2}) compared to CI-OFDM-IM at the cost of the decrease of spectral efficiency by a factor of $\frac{2(1+2G)}{6G} = \frac{5}{6}$. On the other hand, from the BER curve, we see that the diversity gain for symbol detection is the same as that with $G = 1$ in Fig. 3 (a). From the simulation results in Fig. 3, we can claim that OFDM-IM-TD is to improve the diversity gain for index detection, while CI-OFDM-IM can provide a diversity gain for data symbol detection.

[3]As a result, the average BER, denoted by ABER, becomes ABER = BER$(1 - \text{IER}) + \frac{1}{2}$IER (under the assumption that the BER becomes $\frac{1}{2}$ if an inactive index is chosen), which demonstrates the overall performance is strongly dependent on IER and a lower IER is desirable.

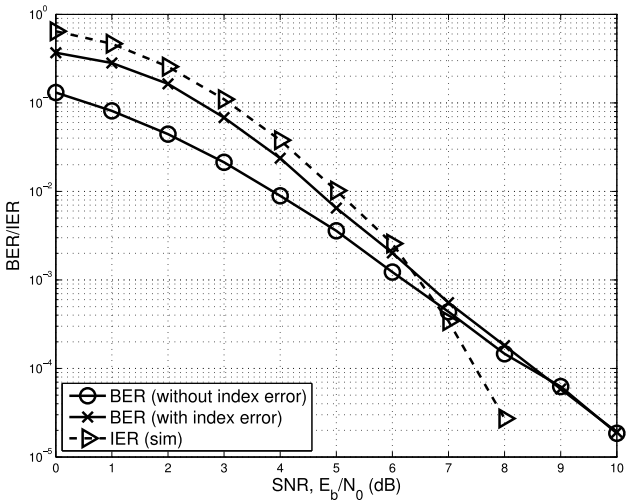

(a)

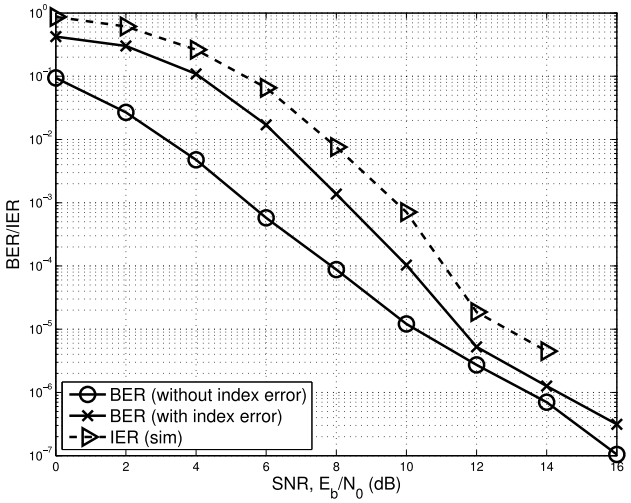

(b)

Fig. 5. Performance of OFDM-IM-TD in terms of IER and coded BER for different values of $\frac{E_b}{N_0} = 6$ when $B = 2048$, $Q = 8$, and $M = 4$: (a) $(K, G) = (16, 8)$; (b) $(K, G) = (32, 4)$.

Fig. 4 shows the IER and BER for various values of G when $N = 4$, $\frac{E_b}{N_0} = 4$ dB, $Q = 2$, and $M = 4$. As G increases, the diversity gain for index detection increases in OFDM-IM-TD (which results in a lower IER) at the cost of the decrease of spectral efficiency, while there is no performance improvement in CI-OFDM-IM.

In Fig. 4, we can also confirm that the increase of G improves the IER, but not the BER in OFDM-IM-TD. Thus, we need channel coding for data symbols as mentioned earlier.

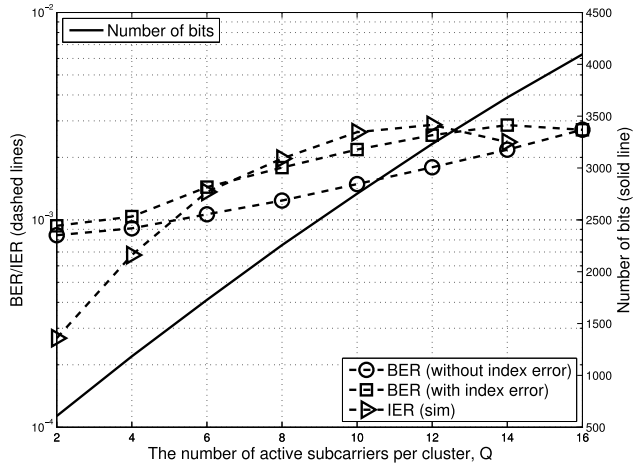

Fig. 6. Performance of OFDM-IM-TD in terms of IER and coded BER for different values of Q when $B = 2048$, $K = 16$, $G = 8$, $M = 4$, and $\frac{E_b}{N_0} = 6$ dB.

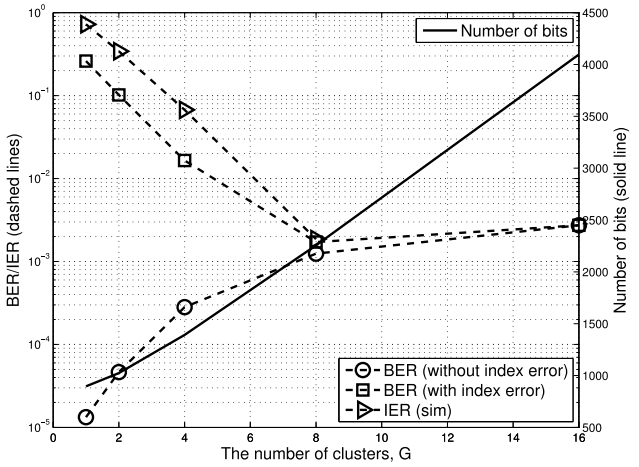

Fig. 7. Performance of OFDM-IM-TD in terms of IER and coded BER for different values of G when $B = 2048$, $K = 16$, $Q = 8$, $M = 4$, and $\frac{E_b}{N_0} = 6$ dB.

B. Simulation Results for Coded Signals

In this subsection, we present simulation results for coded OFDM-IM-TD. We assume that a rate-half convolutional code with a random bit interleaver is used for a BICM transmitter. The generator polynomial of the convolutional code is $(5, 7)$ in octal.

We show the simulation results in Fig. 5 to see the performance of OFDM-IM-TD in terms of IER and coded BER for various values of $\frac{E_b}{N_0}$ when $B = 2048$, $Q = 8$, and $M = 4$. In Fig. 5 (a), we have $G = 8$, which results in a low IER. Thus, we can see that the coded BER with index error (which is the performance of coded OFDM-IM-TD) approaches the coded BER without index error (which is equivalent to the performance of BICM) even at a low $\frac{E_b}{N_0}$ (say 6 dB). However, as shown in Fig. 5 (b), when $G = 4$, the IER is high. Since the coded BER with index error is subject to the performance IER, at a low $\frac{E_b}{N_0}$ (say 6 dB), there is a noticeable gap between the coded BERs with and without index error. However, as $\frac{E_b}{N_0}$ increases, this gap becomes narrower.

Fig. 6 shows the performance for different values of Q when $B = 2048$, $K = 16$, $G = 8$, $M = 4$, and $\frac{E_b}{N_0} = 6$ dB. The number of bits per subblock, $\bar{N}_b$ in (6), increases with Q (when the other parameters are fixed), while the coded BER increases with Q. In addition, as expected, the coded BER is limited by the IER. Note that the coded BER curves (with and without index error) meet at $Q = 16$. Since $L = B/K = 128$ is fixed, we have $N = L/G = 16$. Thus, when $Q = 16$, all the subcarriers are active and IER becomes 0, which makes the coded BER with and without index error the same at $Q = 16$.

Fig. 7 shows the performance for different values of G when $B = 2048$, $K = 16$, $Q = 8$, $M = 4$, and $\frac{E_b}{N_0} = 6$ dB. Note that when $G = 16$, we have $N = 8$, which is the same as Q. Thus, in this case, the IER becomes 0. As the number of bits per subblock, $\bar{N}_b$ in (6), increases with G, the coded BER without index error increases with G. However, since the coded BER with index error depends on the IER, it has a $\cup$-shape in terms of G (the dashed line with $\square$ marks). That is, when G is small, the IER is high. Thus, the coded BER with index error is high.

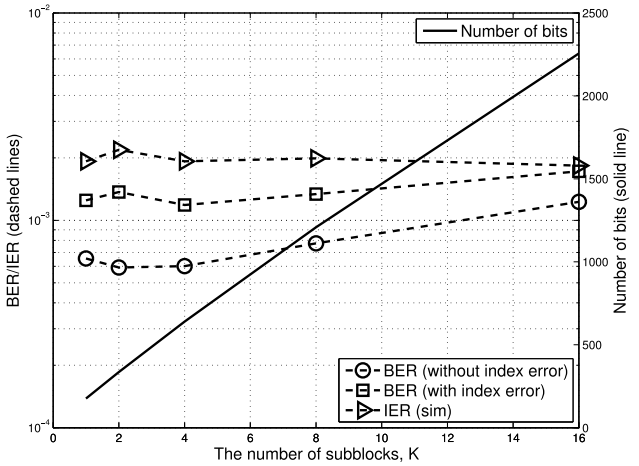

Fig. 8. Performance of OFDM-IM-TD in terms of IER and coded BER for different values of K when $B = 2048$, $G = 8$, $Q = 8$, $M = 4$, and $\frac{E_b}{N_0} = 6$ dB.

However, as G increases, the coded BER with index error can decrease, and for a sufficiently low IER, the coded BER with index error approaches that without index error. As a result, the coded BER with index error has a $\cup$-shape in terms of G.

We present the simulation results in Fig. 8 to see the impact of K on the performance when $B = 2048$, $G = 8$, $Q = 8$, $M = 4$, and $\frac{E_b}{N_0} = 6$ dB. As shown in (7), the number of bits per blocks increases with K, while the coded BER is almost invariant with respect to K. Thus, it is desirable to have a large K when B, G, Q, and M are fixed.

VI. Concluding Remarks

We have proposed a simple but effective transmit diversity scheme for OFDM-IM in this paper and derived the ML approach for active index detection. The proposed scheme was able to provide a high diversity gain for index detection under a frequency-selective fading environment, which can improve the detection performance of active subcarriers. As a result, it was shown that the proposed scheme can have more than 8 dB gain in terms of $\frac{E_b}{N_0}$ at an IER of 10^{-1} (and about 13 dB

gain at an IER of 10^{-2}) compared to an existing transmit diversity scheme for OFDM-IM at the cost of the decrease of spectral efficiency by a factor of $\frac{5}{6}$. Importantly, since the proposed transmit diversity scheme can be easily employed in conjunction with a conventional channel coding scheme for data symbols, coded OFDM-IM together with the proposed transmit diversity could be implemented in a straightforward manner with a good performance under a frequency-selective fading environment.

REFERENCES

[1] R. Y. Mesleh, H. Haas, S. Sinanovic, C. W. Ahn, and S. Yun, "Spatial modulation," *IEEE Trans. Veh. Technol.*, vol. 57, no. 4, pp. 2228–2241, Jul. 2008.

[2] M. Di Renzo, H. Haas, A. Ghrayeb, S. Sugiura, and L. Hanzo, "Spatial modulation for generalized mimo: Challenges, opportunities, and implementation," *Proc. IEEE*, vol. 102, no. 1, pp. 56–103, Jan. 2014.

[3] P. Yang, M. Di Renzo, Y. Xiao, S. Li, and L. Hanzo, "Design guidelines for spatial modulation," *IEEE Commun. Surveys Tuts.*, vol. 17, no. 1, pp. 6–26, 1st Quart., 2015.

[4] J. Jeganathan, A. Ghrayeb, and L. Szczecinski, "Spatial modulation: Optimal detection and performance analysis," *IEEE Commun. Lett.*, vol. 12, no. 8, pp. 545–547, Aug. 2008.

[5] R. Mesleh, M. Di Renzo, H. Haas, and P. M. Grant, "Trellis coded spatial modulation," *IEEE Trans. Wireless Commun.*, vol. 9, no. 7, pp. 2349–2361, Jul. 2010.

[6] J. Choi, "Signal dependent antenna mapping for spatial modulation," in *Proc. IEEE 79th Veh. Technol. Conf. (VTC)*, May 2014, pp. 1–5.

[7] J. Jeganathan, A. Ghrayeb, L. Szczecinski, and A. Ceron, "Space shift keying modulation for MIMO channels," *IEEE Trans. Wireless Commun.*, vol. 8, no. 7, pp. 3692–3703, Jul. 2009.

[8] R. Mesleh, S. S. Ikki, and H. M. Aggoune, "Quadrature spatial modulation," *IEEE Trans. Veh. Technol.*, vol. 64, no. 6, pp. 2738–2742, Jun. 2015.

[9] R. Abu-Alhiga and H. Haas, "Subcarrier-index modulation OFDM," in *Proc. IEEE 20th Int. Symp. Pers. Indoor Mobile Radio Commun.*, Sep. 2009, pp. 177–181.

[10] E. Başar, Ü. Aygölü, E. Panayirci, and H. V. Poor, "Orthogonal frequency division multiplexing with index modulation," *IEEE Trans. Signal Process.*, vol. 61, no. 22, pp. 5536–5549, Nov. 2013.

[11] E. Başar, "Index modulation techniques for 5G wireless networks," *IEEE Commun. Mag.*, vol. 54, no. 7, pp. 168–175, Jul. 2016.

[12] Y. Ko, "A tight upper bound on bit error rate of joint OFDM and multi-carrier index keying," *IEEE Commun. Lett.*, vol. 18, no. 10, pp. 1763–1766, Oct. 2014.

[13] R. Fan, Y. J. Yu, and Y. L. Guan, "Generalization of orthogonal frequency division multiplexing with index modulation," *IEEE Trans. Wireless Commun.*, vol. 14, no. 10, pp. 5350–5359, Oct. 2015.

[14] E. Başar, "Multiple-input multiple-output OFDM with index modulation," *IEEE Signal Process. Lett.*, vol. 22, no. 12, pp. 2259–2263, Dec. 2015.

[15] W. Li, H. Zhao, C. Zhang, L. Zhao, and R. Wang, "Generalized selecting sub-carrier modulation scheme in OFDM system," in *Proc. IEEE Int. Conf. Commun. Workshops (ICC)*, Jun. 2014, pp. 907–911.

[16] D. L. Donoho, "Compressed sensing," *IEEE Trans. Inf. Theory*, vol. 52, no. 4, pp. 1289–1306, Apr. 2006.

[17] E. J. Candès, J. Romberg, and T. Tao, "Robust uncertainty principles: Exact signal reconstruction from highly incomplete frequency information," *IEEE Trans. Inf. Theory*, vol. 52, no. 2, pp. 489–509, Feb. 2006.

[18] C.-M. Yu *et al.*, "Compressed sensing detector design for space shift keying in MIMO systems," *IEEE Commun. Lett.*, vol. 16, no. 10, pp. 1556–1559, Oct. 2012.

[19] S. Kallummil and S. Kalyani, "Combining ML and compressive sensing: Detection schemes for generalized space shift keying," *IEEE Wireless Commun. Lett.*, vol. 5, no. 1, pp. 72–75, Feb. 2016.

[20] J. Choi and Y. Ko, "Compressive sensing based detector for sparse signal modulation in precoded OFDM," in *Proc. IEEE Int. Conf. Commun. Workshops (ICC)*, Jun. 2015, pp. 4536–4540.

[21] Y. S. Cho, J. Kim, W. Y. Yang, and C. G. Kang, *MIMO–OFDM Wireless Communications With MATLAB*. New York, NY, USA: Wiley, 2010.

[22] J. Choi, *Adaptive and Iterative Signal Processing in Communications*. Cambridge, U.K.: Cambridge Univ. Press, 2006.

[23] E. Başar, "OFDM with index modulation using coordinate interleaving," *IEEE Wireless Commun. Lett.*, vol. 4, no. 4, pp. 381–384, Aug. 2015.

[24] H. Sari, G. Karam, and I. Jeanclaude, "Transmission techniques for digital terrestrial TV broadcasting," *IEEE Commun. Mag.*, vol. 33, no. 2, pp. 100–109, Feb. 1995.

[25] M. Z. A. Khan and B. S. Rajan, "Single-symbol maximum likelihood decodable linear STBCs," *IEEE Trans. Inf. Theory*, vol. 52, no. 5, pp. 2062–2091, May 2006.

[26] S. M. Kay, *Fundamentals of Statistical Signal Processing: Detection Theory*. Englewood Cliffs, NJ, USA: Prentice-Hall, 1998.

[27] A. Guillén i Fàbregas, A. Martinez, and G. Caire, "Bit-interleaved coded modulation," *Found. Trends Commun. Inf. Theory*, vol. 5, nos. 1–2, pp. 1–153, 2008.

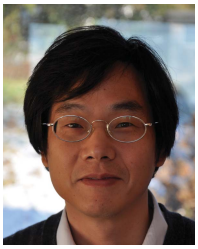

Jinho Choi (SM'02) was born in Seoul, South Korea. He received the B.E. *(magna cum laude)* degree in electronics engineering from Sogang University, Seoul, South Korea, in 1989, and the M.S.E. and Ph.D. degrees in electrical engineering from the Korea Advanced Institute of Science and Technology, Daejeon, South Korea, in 1991 and 1994, respectively. He was a Professor/Chair of Wireless with the College of Engineering, Swansea University, U.K. He is currently a Professor with the Gwangju Institute of Science and Technology. His research interests include wireless communications and array/statistical signal processing. He has authored two books published by Cambridge University Press in 2006 and 2010. He received the 1999 Best Paper Award for Signal Processing from EURASIP and the 2009 Best Paper Award from WPMC (Conference). He is currently an Editor of the IEEE TRANSACTIONS COMMUNICATIONS and served as an Associate Editor or Editor of other journals including the IEEE COMMUNICATIONS LETTERS, the *Journal of Communications and Networks*, the IEEE TRANSACTIONS ON VEHICULAR TECHNOLOGY, and *ETRI Journal*.